

18th International Vacuum Congress (IVC-18)

Research on Thin Film Thickness Uniformity for Deposition of Rectangular Planar Sputtering Target

ZHANG Yichen^a, SONG Qingzhu^{b, *}, SUN Zhulai^b^aNortheastern University, Shenyang 110004, China^bShen Yang Vacuum Technology Institute, Shenyang 110042, China

Abstract

Magnetron sputtering coating is widely applied in the large area deposition, and thin film thickness uniformity, deposition ratio, utilization ratio of target material and other problems in coating industry are paid great attention. As one of the most important parameters for testing sputtering process, the study on the related issues of thin film uniformity is of great theoretical and practical value. The fundamental theory on deposition of sputtering coating is analyzed based on existing theories, and the model of deposition flux that is composed of fast- and slow-moving particles is applied to the rectangular planar magnetron sputtering target. Through the application of Matlab software and the numerical calculation of thin film deposition uniformity of a rectangular planar magnetron sputtering target, it is easy to come to the following conclusions: the thickness uniformity will reduce with the increase of target-substrate distance and with the decrease of erosion zone of the target ends. When the erosion zone of the target ends increases to some extent, the thin film thickness uniformity will become higher with the increase of target-substrate distance and then become lower. There are two tendencies for thin film thickness uniformity with the increase of length-width ratio of target erosion zone, that is, it will become a little lower when the length is a constant, or become higher when the width is a constant. And the thin film thickness uniformity will become lower with the decrease of power and the increase of gas temperature. The deposition rate will become higher with the decrease of target-substrate distance, or the increase of power and gas temperature.

Keywords: Magnetron sputtering; Thin film thickness uniformity; Target-substrate distance; Numerical calculation

1. Introduction

With the development of vacuum coating technology, equipments for coating on planar substrate have been improved greatly with increasingly perfect functions. As the advancement of vacuum coating equipments originates from the perfection of processes and the development of processes originates from the continuous developing of theories, the upgrading of vacuum coating equipments necessitates the perfection of theoretical systems. The uniformity of thin film thickness is one of the important indices to test the equipment performance and product quality. On the basis of existing theories, this paper presents a preliminary study on the thin film thickness distribution of a rectangular planar magnetron sputtering target by use of numerical calculation.

* Corresponding author. Tel.: +0-086-13840146086 ; fax: +0-086-024-24141990 .

E-mail address: songqingzhu_vac@126.com .

2. Modeling of thin film thickness distribution

In magnetron sputtering, due to the influence of gas pressure, deposited particles can be roughly divided into fast-moving particles (not collide) and slow-moving particles (collide). The more detailed study should take other influences into consideration, including gas heated by the collision with sputtered particles, gas inhomogeneous rarefaction effect and thermalization effect of sputtered particles. Meanwhile, due to the processes of particles like moving and re-emission on deposited surface that are caused by the difference between energy state of sputtered particles and physical-chemical state of deposited surface, the re-emission of deposited particles and other factors are also very important^[1-13].

When depositing particles travel in the space between the target and the substrate, they will collide with gas to scatter, and this scattering process is a random event. If mean free path λ_s is taken as characteristic constant, then the relation among λ_s , gas temperature T and pressure P is^[14, 15]:

$$\lambda_s = \frac{kT}{P\sigma} \quad (1)$$

where k is the Boltzmann constant, and σ is the cross-section for momentum transfer.

This paper takes a rectangular planar magnetron sputtering target as the research object, and then the thin film thickness uniformity will be studied based on depositing particle models of fast- and slow- moving particles.

2.1. Thin film thickness distribution model for fast-moving particles

It is typical to express flux density φ_f of the fast atoms at the substrate, a distance ρ from the target as^[3]:

$$\varphi_f = \varphi_d \exp\left(-\frac{\rho}{\lambda_s}\right) \quad (2)$$

$$\varphi_f = \varphi_d \exp(-\delta P\rho) \quad (3)$$

Eq. (2) may be expressed as Eq. (3), where φ_d is given by:

$$\varphi_d = j(r)YS(\theta) \quad (4)$$

where, $j(r)$ is the ion current density, Y is the normal target sputtering yield, $S(\theta)$ is a function of the emission position on the target and the cosine distribution factor, Yamamura et al. proposed a fitting formula of the form^[4, 16, 17, 18]:

$$S(\theta) \approx \cos\theta(1 + \beta \cos^2\theta) \quad (5)$$

where θ is the ejection angle of the sputtered atoms with respect to the surface normal and β is a fitting parameter. δ is dependent on the free path of the atoms, determined by the gas-target combination, normal pressure and the applied power due to gas rarefaction effect.

Using Eq. (3) and from Fig. 1(a), the flux density of the particles sputtered from an element area dA_T of the target onto an element area dA_S of the substrate may be expressed as :

$$d\varphi_f = \varphi_d \exp(-C\rho)dA_T d\Omega / dA_S \quad (6)$$

where $C = \delta P = \lambda_s^{-1}$, $d\Omega = dA_S \cos\theta / \rho^2$, $\cos\theta = z / \rho$. The rectangular target is described by circular cylindrical coordinates easily, $dA_T = r dr d\phi$. The total flux density of the fast moving sputtered particles at the substrate may be obtained by integrating Eq. (6) over the area of the target etch track as:

$$\varphi_f = \iint \frac{j(r)Yz^2(1 + \beta(z/\rho)^2)}{\rho^4} \exp(-C\rho) r dr d\phi \quad (7)$$

Using the geometry of Fig. 1 (a), $\rho = (z^2 + r^2 + R^2 - 2rR\cos\phi)^{1/2}$. The integral domain is the area of the etch track. Eq. (7) can be integrated numerically for the depositing rate of the fast-moving particles.

2.2. Thin film thickness distribution model for slow-moving particles

Slow-moving particles are the scattered ones which are transported by diffusion. It is typical to apply the distributed source model to determine slow-moving ones^[19]. Petrov et al. believed that the sputtered atoms, however, were not thermalized in a single collision event. The average distance L traveled by the atoms in the initial direction before being thermalized. The distance L is proportional to the thermal mean free path with a factor which is a function of the ratio of the mass of the gas and the target atom, and the energy of the sputtered atom. From Fig. 1(b), the total particles emitted from an element area of the target, which has reached a point, P , without scattering is^[3]:

$$\phi_f = j(r)YS(\theta)rdrd\varphi d\Omega \exp(-C\rho) \tag{8}$$

If pressure were zero, the total particles at P would be:

$$\phi_0 = j(r)YS(\theta)rdrd\varphi d\Omega \tag{9}$$

Thus, the number of particles scattered from the depositing flux is:

$$\phi_s = j(r)YS(\theta)rdrd\varphi d\Omega [1 - \exp(-C\rho)] \tag{10}$$

The density in atoms $\text{cm}^{-3} \text{s}^{-1}$ of the particles scattered into an element volume, $dV=d\Omega\rho^2d\rho$, from the flux emitted from the target element is given by:

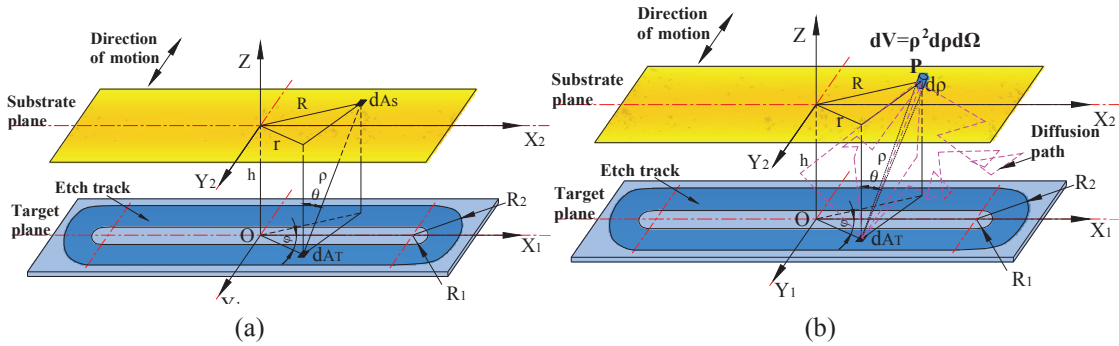


Fig. 1 System geometry used in modeling the flux of (a) fast- and (b) slow-moving particles from a planar target onto a planar substrate.

$$\frac{d\phi_s}{dV} = \frac{Cj(r)YS(\theta)}{\rho^2} \exp(-C\rho)rdrd\varphi \tag{11}$$

The density of the diffusing source in an element volume is n :

$$n = \frac{d\phi_s}{dV} = \frac{Cj(r)YS(\theta)}{\rho^2} \exp(-C\rho)rdrd\varphi$$

Ekpe et al. transform Eq. (11) from the source density of a conservation equation and Fick's first law^[4]:

$$\frac{d\phi_s}{dV} = \frac{\phi_s(\rho + d\rho) - \phi_s(\rho)}{d\rho} = \frac{d}{d\rho} [\phi_s(\rho)] \tag{12}$$

$$\frac{d}{d\rho} [\phi_s(\rho)] = \frac{Cj(r)YS(\theta)}{\rho^2} \exp(-C\rho)rdrd\varphi \tag{13}$$

In a certain range, when the system, where the research objects (a certain number of particles) are in, keeps its number of particles constant, that is, particles into the system equal particles out of it, it will meet Fick's first law, as shown in Fig. 2. The number of molecular passing an element area in an element time is:

$$\phi_s(\rho) = -D \frac{dn}{d\rho} \tag{14}$$

where D is the diffusion coefficient. These particles derive from the etching unit of the whole etching zone, and they diffuse in all directions with the solid angle 4π of the point. Therefore, Ekpe et al. gave the equation of the flux diffusing in a given direction:

$$\varphi_s = \frac{zC}{4\pi} \times \int_{r_1}^{r_2} \int_{\theta_1}^{\theta_2} \int_0^{+\infty} \frac{j(r)Yrdrd\varphi}{\rho^3} (1 + \beta(z/\rho)^2) \exp(-C\rho)d\rho \quad (15)$$

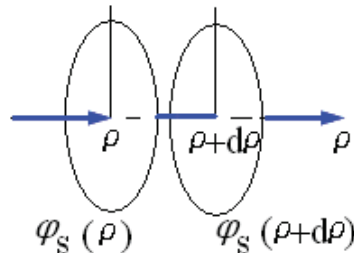


Fig. 2 The diffusion model of Fick's first law for the flux of slow-moving particles

The improper integral of ρ is divergent at lower limit. A parameter which can describe the transport process is needed to define the lower limit. $L \{ \lambda(\text{atom's mean free path}), M(\text{gas' mass})/M(\text{atom's mass}), E(\text{atom's energy}) \}$ may be the parameter given by Pertrov et al. The function of L can be induced through experiments. A parameter Q is also needed to define the upper limit and depends on the free path of the sputtered atoms, which is determined by the gas-target combination and energy, and so on. All diffusing particles do not reach the substrate by the same path way. Under the integrability condition of ρ , either L or Q is the function of ρ . The result of the improper integral should be the function of ρ . From Fig. 1(b), the total diffusing flux is directly deduced by Fick's first law in this paper:

$$\varphi_s(\rho) = -D \frac{dn}{d\rho} = D \frac{Cj(r)YS(\theta)}{\rho^3} (\rho C + 2) \exp(-C\rho)rdrd\varphi \quad (16)$$

It is easy for slow-moving particles to re-emit into the discharge space after depositing on the substrate due to lower energy. The deposition rate is the exclusion of the re-emission part. The total diffusing flux at the point P, due to the emitted flux from all the target elements, is:

$$\varphi_s = \frac{q}{4\pi} \times \iint \frac{z^2 DCj(r)Y(1 + \beta(z/\rho)^2)}{\rho^5} (\rho C + 2) \exp(-C\rho)rdrd\varphi \quad (17)$$

Where q is the coefficient of deposition efficiency for the slow-moving particles^[20,21]. Generally, the value of q is below 0.5, and the value is 0.1 in this paper. Eq. (17) can be integrated numerically for the total flux of slow-moving particles.

The total depositing particles at the substrate is the sum of the fast-moving ones expressed in Eq. (7) and the slow-moving ones expressed in Eq. (17):

$$\varphi_{total} = \varphi_f + \varphi_s \quad (18)$$

The total depositing particles are divided into the fast- and slow-moving ones approximately. In fact, after collision some of the particles reach the substrate with high energy and do not diffuse. Moreover, there is not the only form of diffusion^[20,21].

3. Model Application

The thin film thickness uniformity is under the influence of geometric parameters: target- substrate distance, temperature, gas pressure, electromagnetic and other factors. For the target, it is important to define the geometric parameters of erosion zone (etch track), for they are directly determine the overall trend of thin film deposition. To simplify the model, it is necessary to propose the following hypotheses: the features of erosion zone and the

dynamic characteristics of particles in the depositing process are consistent, that is, the sputtering condition, current density, emission and transportation of sputtered particles are consistent; the erosion zone is flat. Generally, the shape of the zone is the function of time. When target-material is eroded, it will present complicated three-dimensional spatial surface macroscopically.

As the actual size will be confined to the computing time and mesh scale in calculating, the substrate size is designed as 200mm×40mm and placed right to the target surface. For the size of the geometry of the zone, please refer to Fig. 3.

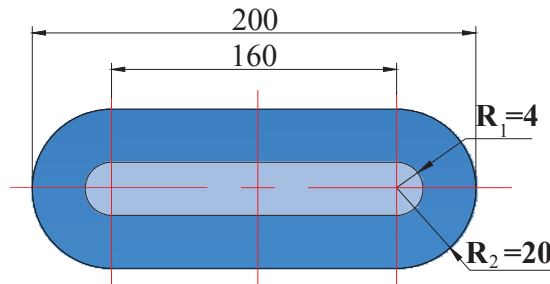


Fig. 3 The geometry of the erosion zone

The selection of parameters: this paper takes copper Cu as the target-material, and argon Ar as working gas. For the value of $\beta^{[4]}$, when the ion incident energy is 100, 600, 1000 and 5KeV respectively, the corresponding value of β is -0.611, 0.284, 0.603 and 1.25; when the value of β is 0, the distribution of emitted particles is the usual cosine distribution.

Usually the energy of the sputtered copper atoms is lower than 10eV ^[14]. Therefore, the corresponding momentum collision section is approximately taken as $4 \times 10^{-20} \text{ m}^{2[22, 23]}$, and the mean free path λ_{Cu} for copper atoms is:

$$\lambda_{Cu} = \frac{kT}{P\sigma} = 3.45 \times 10^{-4} \times \frac{T}{P} \text{ m}$$

The energy of the copper atoms that are away from the target-surface is approximate to 10eV; the variation range of T is 300~400K. For the variation ranges of P and λ_{Cu} are 1~5Pa and 21~138mm, respectively. The programming calculation is obtained by mathematical software MATLAB. The study on the uniformity of deposition rate is realized through the study on the distribution curve of the deposition rate on the substrate, which is an indirect study on the thin film thickness uniformity.

3.1. Thickness distribution of fast-moving particles

Assuming that the change of target substrate will not influence other factors greatly, including pumping speed and density distribution of spatial particles, that is, it will not influence the parameters of the function expression for the deposition rate. This paper only takes the relative movement of the substrate to the target into consideration. The values of β that corresponds to the incident ion energy are taken as 0, 0.284, 0.603, the sputtering yield Y is taken as 1.5 atoms/ion, the current density is 2 mA/cm², and λ_{Cu} is 40mm.

Taken the length percent of uniform deposition zone as longitudinal axis, that is, the ratio between the length of uniform deposition zone on the substrate and the substrate length is taken as an important measurement to judge the thin film thickness uniformity under the condition of different target-substrate distance (lateral axis), the uniform deposition zone mentioned in this paper is the zone whose thin film thickness non- uniformity is lower than 5%. Following is the verification of the change of target-substrate distance from 30mm to 80mm. Through numerical integration calculation, different results will be obtained. From Fig. 4, it is easy to notices that when the substrate moves relatively to the target and the distance changes from 30mm to 80mm, the length percent decreases accordingly. The conclusion that thin film thickness uniformity will rise with the decrease of target-substrate distance made by Gencoa Inc. is consistent with the conclusion of this paper^[24], as Fig. 5(a) shows.

Similarly, as Fig. 6 shows, when λ_{Cu} has different values, the functional relationship between target-substrate distance and the length percent is different. The general trend presented in Fig. 6 is similar to that of Fig. 4, that is, with the increase of target-substrate distance the length percent will decrease.

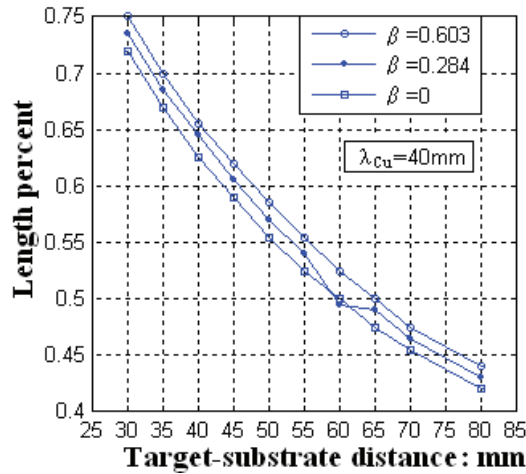


Fig. 4 The length percent at different target-substrate distance

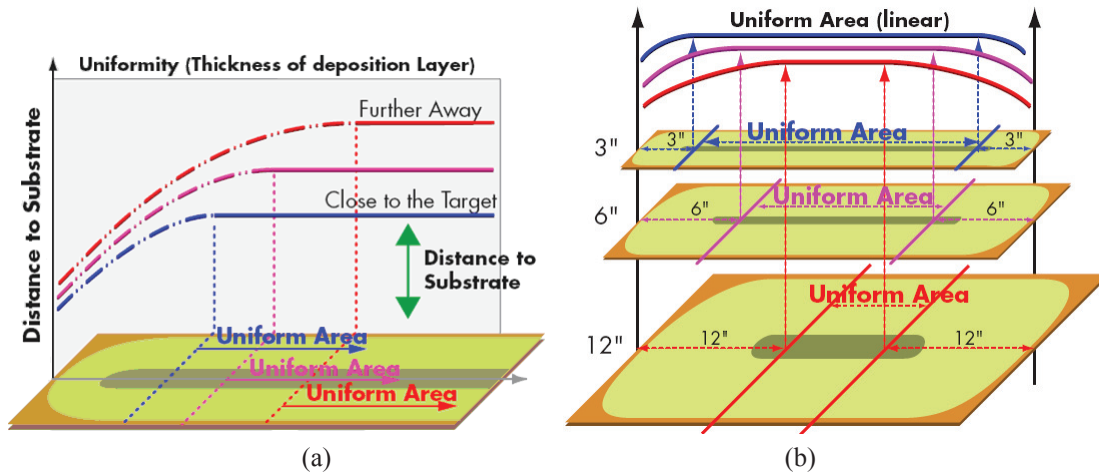


Fig. 5 The relationships between the deposition uniformity and the target-substrate distance (a) or the ratio of the length and width of the erosion zone from Gencoa Inc.

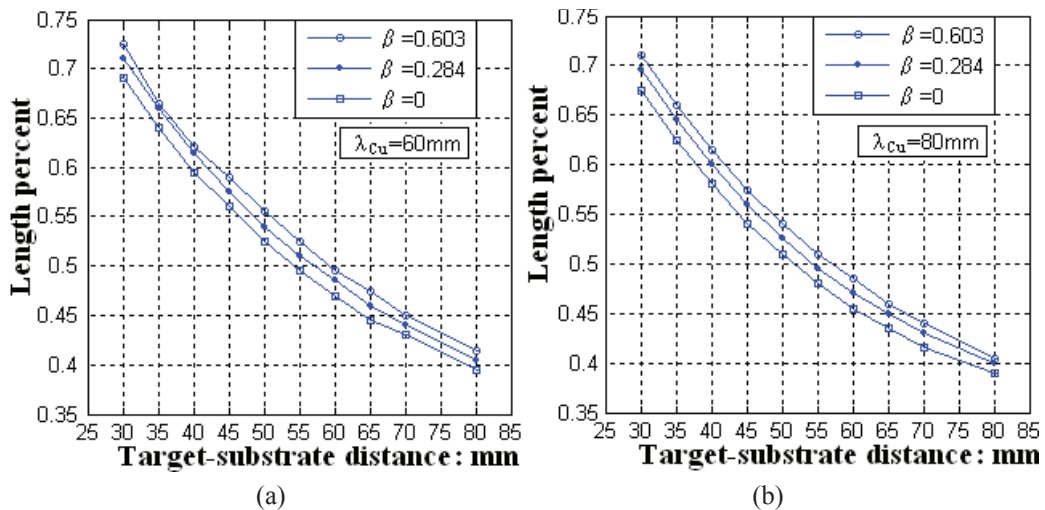


Fig. 6 The variation of the uniform deposition length with different target-substrate distance at different conditions (a) and (b)

It is generally believed that the thin film thickness uniformity of the circle planar magnetron target will rise with the increase of target-substrate distance, while its deposition rate will decrease accordingly. However, for the

rectangular planar magnetron target, it is not easy to copy the conclusion of the circle planar magnetron target, which can be proved by the conclusions of this paper and other published papers.

When incident ion energy and λ_{Cu} are fixed values, the influence of the end erosion zone on thin film thickness uniformity will be observed, where β is 0.284, and λ_{Cu} is 60mm, as Fig. 7 shows. Through calculation it is known that the proper decrease of the end erosion zone will make thickness uniformity decrease as well. As this geometric structure of erosion zone is easy to cause the inhomogeneous etching at end erosion zone, it should be avoided. Conversely, the appropriate increase of end erosion zone will cause the uniformity to increase. Meanwhile, when it reaches to certain value (according to the geometric parameter of this paper, the offset Δ is -14mm), shown as Fig. 7(b), the uniformity will increase first and then decrease with the increase of target-substrate distance.

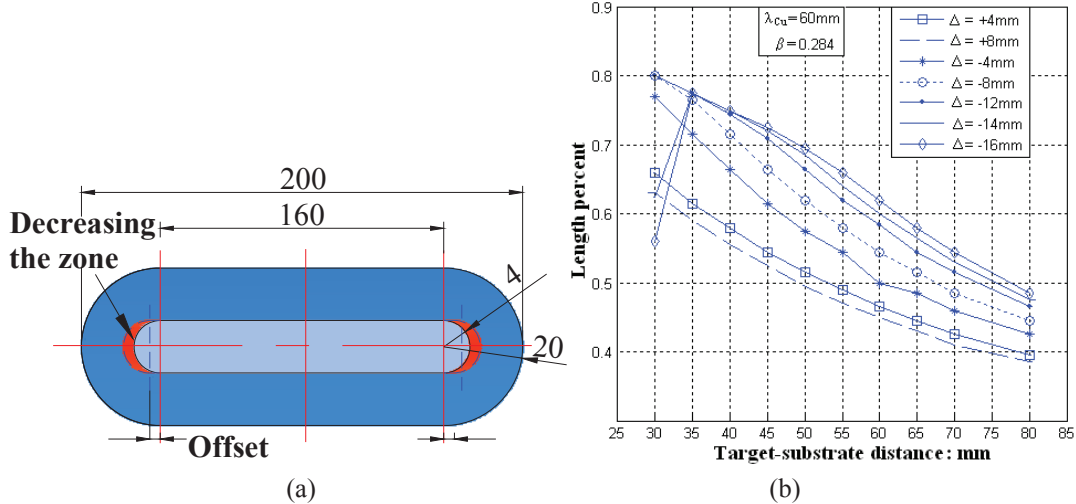


Fig. 7 The variation on uniform deposition length at different offsets of the erosion zone (a) and the relative value of the uniform deposition length (b)

The further research needs to consider how to design the geometric model parametrically so that the erosion zone can be simplified as the following “standard model”. This model can be set by three parameters, shown as Fig. 8, those are R_1 , R_2 and L , which can be correspondingly described as R_1 , mR_1 , nR_1 , $m > 1$, and $n \geq 0$. When $n = 0$, the erosion zone are concentric rings. The ratio S between the total length and width is $(1+n/m)$.

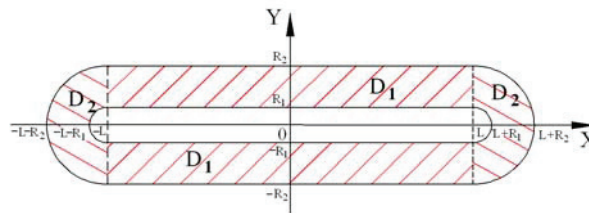


Fig. 8 The geometry used in the parameterization of the erosion zone

The size of the geometric structure, namely, R_1 is 4mm, m is 5, n is 20, S is 3. Given β is 0.284, λ_{Cu} is 60mm, and R_1 is 4mm, when n is 20, m is 3 or 4; when m is 5, n is 22, 24 and 30. In these two situations, the value of S will increase. The research is that how the increased value of S has influence on the thin film uniformity. The size of the substrate will change accordingly, such as, when m is 3, the size is 184mm \times 24mm.

It is easy to conclude that when the value of n is not changed and the value of m is decreased, the uniformity will decrease as well; when the value of m is not changed and the value of n is increased, the uniformity will increase clearly. However, their relation is not a simple linear one, please refer to Fig. 6(a) and Fig. 9.

The results above indicate that as the way of the increase of length or width is different, the change of thin film thickness uniformity is different. As Fig. 5(b) shows, the conclusion that the uniformity will rise with the increase of length-width ratio of erosion zone made by Gencoa Inc. is consistent with the conclusion of this paper, yet it does not point out the way.

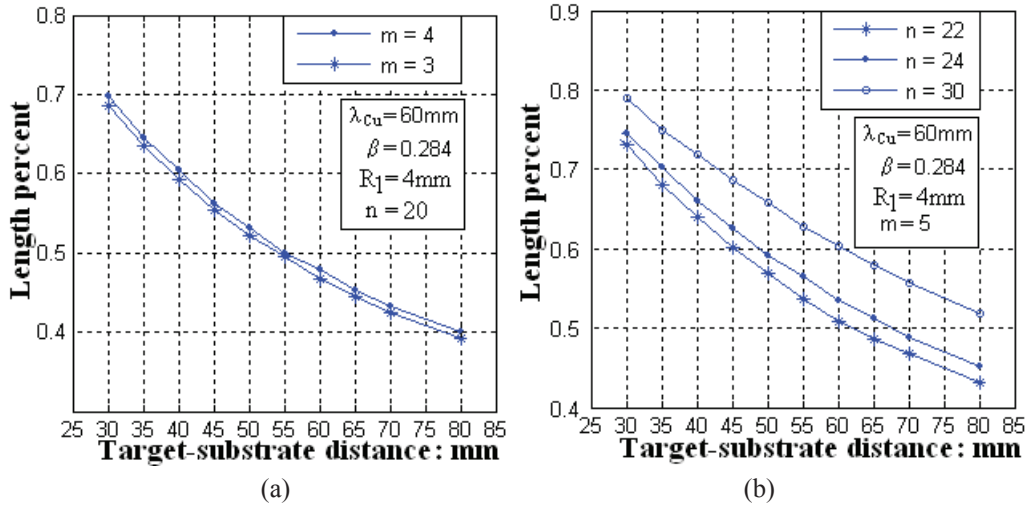


Fig. 9 The variation on uniformity with the ratio of length / width of the erosion zone on constant n (a) and constant m (b) conditions

3.2. Thickness distribution of slow-moving particles

The slow-moving particles for deposition are moving by diffusing. Generally, the uniformity of slow-moving particles is better than that of fast-moving ones. This paper only considers the features of slow-moving particles when β is 0.284, and λ_{cu} is 60mm. As Fig. 10 shows, through the calculation results, it is easy to come to the conclusion that in the same condition the uniformity of slow-moving is better. It is also shows that the length percent in the uniform deposition zone will decrease with the increase of target-substrate distance, which is the same with the deposition features of fast-moving ones, and accords with the actual situation^[3,4].

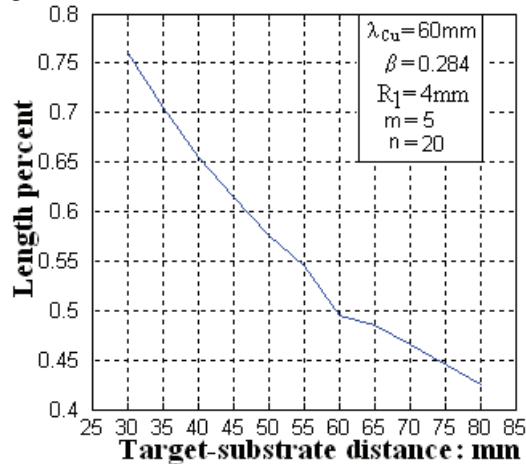


Fig. 10 The deposition uniformity of the flux of slow-moving particles

3.3. Thickness distribution of the total particles

The total thickness distribution needs to calculate both fast- and slow- moving particles, as Fig. 11 shows. The fast ones may dominate at low pressure and will decrease with the increase of pressure, while the slow ones will dominate in the high-pressure regime. With the further increase of pressure, their proportions will tend to change gently. Assuming the current is constant, when the value of β is reduced from 0.603 to 0.284 or 0, the power will reduce accordingly, which conforms with the fact that the deposition rate will reduce with the decrease of power.

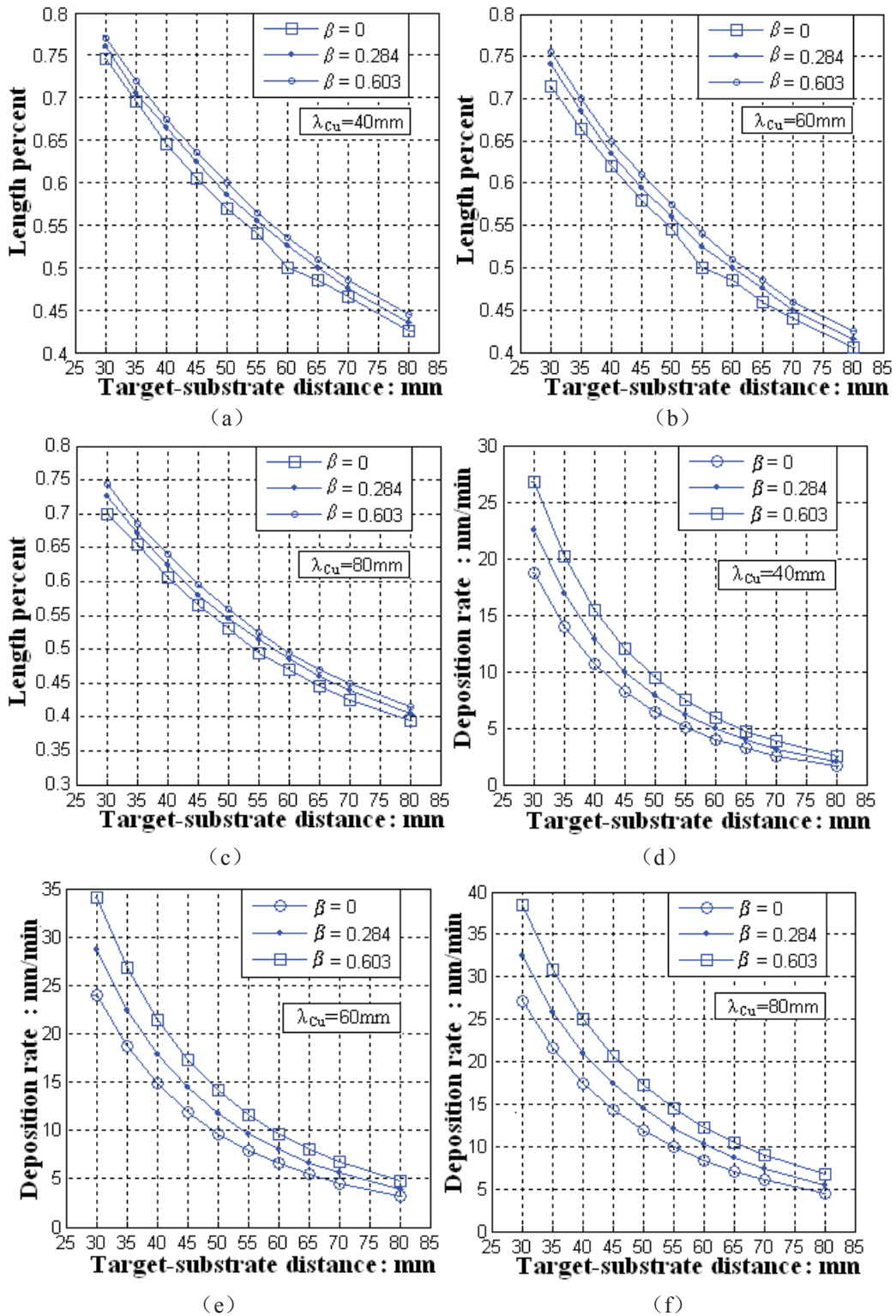


Fig. 11 The variation of the uniform deposition length percent (a), (b), (c) and the deposition rate (d), (e), (f) with different conditions for the total deposition flux

When λ_{Cu} is changed from 80mm to 40mm, the pressure will increase or the temperature will decrease accordingly, which conforms with the conclusion that the deposition rate will decrease with the increase of pressure correspondingly^[3, 4].

As the rise of gas temperature that is caused by the collision of sputtered particles in the discharge space is inhomogeneous^[25], and the process like inhomogeneous gas rarefaction density cannot be described directly and accurately by existing mathematical model, the numerical calculation is usually obtained by the basic physical model like the collision model. Therefore, the spatial distribution function of gas temperature and density can be obtained, which are the immediate results for further calculation. This paper does not take the process into consideration, hence there exists deviation between model and actual situation to some extent.

From the calculation results discussed above, we can conclude that the distribution of deposition rate is greatly influenced by the size of the erosion zone, while the power of magnetron target, target-material and pressure will not influence the general distribution trend for the distribution. Unlike the circle planar magnetron sputtering target, although the thin film deposition uniformity of the rectangular planar magnetron sputtering target will not rise with the increase of target distance, its deposition rate will decrease with the increase of target distance. The calculation result conforms to the actual situation.

4. Conclusion

Through the discussion of thin film thickness distribution theory, this paper presents the calculation results for the thin film thickness uniformity of rectangular planar target with detailed comparison of the influence of geometric parameters, target-substrate distance, incident ion energy and other parameters. The calculation results are tested indirectly and consistent with the actual situation: the thickness uniformity will reduce with the increase of target-substrate distance and with the decrease of erosion zone of the target ends. When the erosion zone of the target ends increases to some extent, the uniformity will become higher with the increase of target-substrate distance and then become lower. There are two tendencies for thin film thickness uniformity with the increase of length-width ratio of target erosion zone, that is, it will become a little lower when the length is a constant, or become higher when the width is a constant. And the thin film thickness uniformity will become lower with the decrease of power and the increase of gas temperature. The deposition rate will become higher with the decrease of target-substrate distance, or the increase of power and gas temperature.

References

- [1] K. Meyer, I. K. Schuller, C. M. Falco. Thermalization of sputtered atoms [J], *J. Appl. Phys.*, 1981, 52(9): 5803-5805.
- [2] T. Motohiro. Applications of Monte Carlo simulation in the analysis of a sputter-deposition process [J], *J. Vac. Sci. Technol. A*, 1986, 4(2): 189-95.
- [3] I. Petrov, I. Ivanov, V. Orlinov, etc. Comparison of magnetron sputter deposition conditions in neon, argon, krypton, and xenon discharges [J], *J. Vac. Sci. Technol. A*, 1993, 11(5): 2733-2741.
- [4] S. D. Ekpe, L. W. Bezuidenhout, S. K. Dew. Deposition rate model of magnetron sputtered particles [J], *Thin Solid Films*, 2005, 474(1-2): 330-336.
- [5] T. Yagisawa, T. Makabe. Modeling of dc magnetron plasma for sputtering: Transport of sputtered copper atoms [J], *J. Vac. Sci. Technol. A*, 2006, 24(4): 908~913.
- [6] S. M. Rosnagel. Gas density reduction effects in magnetrons [J], *J. Vac. Sci. Technol. A*, 1988, 6(1): 19-24.
- [7] D. W. Hoffman. A sputtering wind [J], *J. Vac. Sci. Technol. A*, 1985, 3(3): 561-566.
- [8] G. M. Turner. Monte Carlo calculations of gas rarefaction in a magnetron sputtering discharge [J], *J. Vac. Sci. Technol. A*, 1995, 13(4): 2161-2169.
- [9] F. Jimenez, S. D. Ekpe, S. K. Dew. Inhomogeneous rarefaction of the process gas in a direct current magnetron sputtering system [J], *J. Vac. Sci. Technol. A*, 2006, 24(4): 1530-1534.
- [10] A. Belkind, F. Jansen. Anode effects in magnetron sputtering [J], *Surface and Coatings Technology*, 1998, 99(1-2): 52-59.
- [11] K. S. Fancey. A coating thickness uniformity model for physical vapour deposition systems: overview [J], *Surface and Coatings Technology*, 1995, 71(1): 16-29.

- [12] K. S. Fancey. A coating thickness uniformity model for physical vapour deposition systems: further analysis and development [J], *Surface and Coatings Technology*, 1998, 105(1-2): 76-83.
- [13] A. Kuzmichev, I. Goncharuk. Simulation of the sputtered atom transport during a pulse deposition process in single- and dual-magnetron systems [J], *IEEE Trans. Plasma Sci.*, 2003, 31(5): 994-1000.
- [14] M. L. Escrivão, A. M. C. Moutinho, M. J. P. Maneira. Planar magnetron glow discharge on copper: empirical and semiempirical relations [J], *J. Vac. Sci. Technol. A*, 1994, 12(3): 723-726.
- [15] T. Smy, L. Tan, S. S. Winterton, et al. Simulation of sputter deposition at high pressures [J], *J. Vac. Sci. Technol. A*, 1997, 15(6): 2847-2853.
- [16] Y. Yamamura, H. Tawara. Energy dependence of ion-induced sputtering yields from monatomic solids at normal incidence [J], *Atomic Data and Nuclear Data Tables*, 1996, 62(2): 149-253.
- [17] T. Yagisawa, T. Makabe. Modeling of dc magnetron plasma for sputtering: Transport of sputtered copper atoms [J], *J. Vac. Sci. Technol. A*, 2006, 24(4): 908-913.
- [18] S. M. Rossnagel, H. R. Kaufman. Current–voltage relations in magnetrons [J], *J. Vac. Sci. Technol. A*, 1988, 6(2): 223-239.
- [19] G. Ecker, K. G. Emelús. Cathode sputtering in glow discharges [J], *Proc. Phys. Soc. B*, 1954, 67: 546-552.
- [20] J. H. Keller, R. G. Simmons. Sputtering process model of deposition rate [J], *IBM J. Res. Develop.*, 1979, 23(1): 24-32.
- [21] L. I. Maissel, R. E. Jones, C. L. Standley. Re-emission of Sputtered SiO₂ during growth and its relation to film quality [J], *IBM J. Res. Develop.*, 1970, 14(2): 176-181.
- [22] R. S. Robinson. Energy binary collisions in rare gas plasmas [J], *J. Vac. Sci. Technol. A*, 1979, 16(2): 185-188.
- [23] W. D. Westwood. Calculation of deposition rates in diode sputtering systems [J], *J. Vac. Sci. Technol. A*, 1978, 15(1): 1-9.
- [24] <http://www.genco.com>.
- [25] T. P. Drüsedau. Gas heating and throw distance for the sputter deposition of aluminum and tungsten [J], *J. Vac. Sci. Technol. A*, 2002, 20(2): 459-466.